Article

J. Mex. Chem. Soc. **2025**, *69*(4)
Regular Issue

ISSN-e 2594-0317

Fenugreek as a Potential Antiviral Agent against Crimean-Congo Hemorrhagic Fever Virus: an In-depth Theoretical Analysis

Sumit Kumar*, Ravindra Kumar, Nagendra Kumar

PG Department of Chemistry, Magadh University, Bodh Gaya-824234.

***Corresponding author:** Sumit Kumar, email: sumitkrmgr@gmail.com

Received October 27th, 2024; Accepted March 10th, 2025.

DOI: http://dx.doi.org/10.29356/jmcs.v69i4.2384

Abstract. Fenugreek is widely known for its important medicinal, nutritional, and culinary applications, offering antipyretic, anti-inflammatory, and antiviral effects. Its antiviral properties make it particularly interesting for addressing viruses like Crimean-Congo Hemorrhagic Fever Virus (CCHFV). Given the lack of approved treatments for CCHFV and the virus's high fatality rate, it demands urgent attention. The nucleoprotein of CCHFV, a critical factor in the virus's replication process, has been identified as a promising target for the development of antiviral therapies. This study aimed to discover inhibitors of this protein through virtual screening. A combination of docking studies and molecular dynamics simulations was employed to screen active compounds from fenugreek for their ability to inhibit the nucleoprotein. Given that CCHFV is classified as a biosafety level-4 pathogen by the World Health Organization (WHO), making it difficult to study in conventional laboratories, in-silico methods provide a safe and efficient alternative for identifying potential inhibitors. Based on the results of molecular docking and dynamic simulations, Diosgenin, Tigogenone, and Vicenin-2 are proposed as potential inhibitors of the CCHFV nucleoprotein. These findings suggest that fenugreek constituents could be promising leads in the development of antiviral therapies for CCHFV.
Keywords: Fever; diosgenin; tigogenone; vicenin; antiviral.

Resumen. El fenogreco (Trigonella foenum-graecum) es conocido por sus importantes aplicaciones medicinales, nutricionales y culinarias, ofreciendo efectos antipiréticos, antiinflamatorios y antivirales. Estas últimas lo hacen particularmente interesante para enfrentar virus como el de la Fiebre Hemorrágica de Crimea-Congo (CCHFV, por sus siglas en inglés). Dada la ausencia de tratamientos aprobados para el CCHFV y su alta tasa de mortalidad, se requiere una atención urgente. La nucleoproteína del CCHFV, un factor crítico en el proceso de replicación del virus ha sido identificada como un objetivo prometedor para el desarrollo de terapias antivirales. Este estudio tuvo como objetivo descubrir inhibidores de esta proteína mediante cribado virtual. Se empleó una combinación de estudios de acoplamiento molecular y simulaciones de dinámica molecular para evaluar la capacidad de compuestos activos del fenogreco para inhibir la referida nucleoproteína. Dado que el CCHFV está clasificado por la Organización Mundial de la Salud (OMS) como un patógeno de nivel de bioseguridad 4, se dificulta su estudio en laboratorios convencionales, por lo que los métodos in silico ofrecen una alternativa segura y eficiente para la identificación de posibles inhibidores. Con base en los resultados del acoplamiento molecular y las simulaciones dinámicas, se proponen a la diosgenina, la tigogenona y la vicenina-2 como posibles inhibidores de la nucleoproteína del CCHFV. Estos hallazgos sugieren que los componentes del fenogreco podrían constituir candidatos prometedores en el desarrollo de terapias antivirales contra el CCHFV.
Palabras clave: Fiebre; diosgenina; tigogenona; vicenina; antiviral.

Introduction

Fenugreek (also known as Trigonella foenum-graecum) is a plant belonging to the Fabaceae family, widely used for its medicinal properties, nutritional value, and culinary uses.[1] Native to the Mediterranean region, southern

J. Mex. Chem. Soc. **2025**, *69*(4)
Regular Issue

ISSN-e 2594-0317

Europe, and western Asia, fenugreek seeds and leaves have been traditionally used in various forms, such as spices, food supplements, and herbal remedies. Fenugreek seeds and leaves are commonly used in Middle Eastern, Indian, and Mediterranean cuisine. Its seeds have a slightly bitter taste and are used in spice blends like curry powder.

Fenugreek has been traditionally used in many cultures to manage fever, inflammation, and symptoms of viral infections. Although clinical studies on fenugreek's antiviral effects are limited, it is known to possess certain compounds that contribute to its antipyretic, anti-inflammatory, and antiviral properties. [2,3]

Fenugreek has been used in traditional medicine to reduce fevers.[4] The seeds, when boiled into a tea or decoction, are believed to help lower body temperature, soothe inflamed tissues, and boost immune function.[5] This effect is thought to be related to its anti-inflammatory properties, which may help in managing fever as part of the body's inflammatory response to infections. Although specific studies on fenugreek's antiviral activity are not extensive,[6] it has shown promising effects in traditional treatments against viral infections. Its bioactive compounds can enhance the immune system, which helps the body fight viral pathogens. Fenugreek contains flavonoids and polyphenols, which have been known to possess antiviral properties. These compounds may inhibit the replication of viruses, reducing the severity of infections. Fenugreek has also demonstrated benefits in reducing symptoms associated with viral respiratory infections, such as cough, congestion, and sore throat. It is sometimes used as a herbal remedy for managing flu symptoms. Fenugreek's anti-inflammatory compounds, such as saponins and alkaloids, help reduce inflammation in the body. This can be beneficial in managing the symptoms of viral infections, which often involve inflammation of tissues, fever, and other systemic responses. [7,8]

The health benefits of fenugreek are attributed to its diverse chemical composition, which includes Amino Acids, Alkaloid, Saponins, Fibers, Flavonoids and Polyphenols, Vitamins and Minerals.[9, 10] 4-Hydroxyisoleucine, amino acid in fenugreek has been studied for its role in enhancing insulin secretion, which makes fenugreek potentially useful in managing diabetes.[11] However, its impact on viral diseases is not directly established. Trigonelline, a key alkaloid in fenugreek, is known for its potential health benefits, including blood sugar regulation and anti-inflammatory properties.[12] Fenugreek contains various saponins, which are known to possess antioxidant, anti-inflammatory, and immune-modulating properties. Diosgenin, a specific saponin found in fenugreek, is used as a precursor in the synthesis of steroid hormones and has shown potential anticancer and anti-inflammatory effects.[13] Quercetin is a well-known flavonoid with strong antioxidant and antiviral activity.[14] Fenugreek is rich in both soluble and insoluble fibers, which contribute to its use in managing conditions like high cholesterol, blood sugar regulation, and digestive health. Fenugreek seeds contain significant amounts of vitamin C, vitamin A, iron, calcium, and magnesium, all of which support immune function, making it a useful supplement for boosting immunity during illness.

Crimean-Congo Hemorrhagic Fever Virus (CCHFV) is a tick-borne virus that causes Crimean-Congo Hemorrhagic Fever (CCHF), a severe viral disease in humans.[15-17] It belongs to the family Nairoviridae and is primarily transmitted through the bites of infected Hyalomma ticks, or by direct contact with blood or tissues from infected animals or humans.[15, 18-20] Symptoms of Crimean-Congo Hemorrhagic Fever can be severe and may include High fever, headaches, muscle pain, dizziness at initial phase.[17,21-23] After several days, severe bruising, nosebleeds, and uncontrolled bleeding from injection sites or internal organs may occur including Petechiae (small red or purple spots on the skin), bleeding from gums, and bloody vomit or stools. Eventually, organ failure (liver, kidneys) and shock can occur in severe cases. Mortality rates range from 10-40%, depending on timely medical intervention. [15,24]

In this study, the interactions between various active compounds derived from fenugreek and the Crimean-Congo Hemorrhagic Fever Virus (CCHFV) protein were thoroughly investigated to gain a deeper understanding of the molecular mechanisms underlying protein-ligand interactions. Here the CCHFV nucleoprotein is mainly studied. The nucleoprotein is essential for viral genome encapsidation, replication, and transcription, making it a critical component for viral survival. Targeting the nucleoprotein can disrupt these processes, hindering viral propagation. Additionally, inhibitors designed to interact with the nucleoprotein could prevent its interaction with RNA or other viral components, thereby offering a promising antiviral strategy against CCHFV. This aspect will be incorporated into the manuscript to strengthen the discussion on potential therapeutic targets. This was achieved through an integrated approach utilizing both Molecular Docking and Molecular Dynamics (MD) simulations. Molecular Docking helped predict the preferred binding orientations and affinities of the fenugreek constituents within the CCHFV protein's active sites, while MD simulations were employed to monitor the stability and dynamic behavior of these interactions over time. Together, these computational techniques provide valuable insights into how these compounds may inhibit the CCHFV protein, potentially paving the way for future antiviral drug development.

J. Mex. Chem. Soc. **2025**, *69*(4)
Regular Issue

ISSN-e 2594-0317

Computational details

Structural detail

A total of seventeen distinct compounds derived from fenugreek were selected for computational analysis. These molecules are composed of hydrogen (H), carbon (C), oxygen (O), and nitrogen (N) atoms. The chemical structures of these seventeen constituents are depicted in Fig. 1.

Preparation of the target structure for docking

The crystal structure of the Crimean–Congo hemorrhagic fever virus nucleoprotein (CCHFV N) in its monomeric form was obtained from the Protein Data Bank (PDB) under the identifier 4AQG [19]. Upon inspection, the structure was analyzed for any missing side chains or amino acids. It was found that eleven residues between Asn183 and Ser194 were absent from the structure, and these were subsequently modeled using the SWISS-MODEL server.[25,26]

Additionally, sequence alignment was performed using EMBOSS Needle, which compares two input sequences and generates an optimal global sequence alignment, outputting the results to a file (see Fig. S1) .[27] The alignment, visualized in Fig. S1, was computed using the Needleman-Wunsch algorithm, ensuring the best possible match (including gaps) over the full length of the sequences.[28] Preparation of the docked entity: 3D structures of important constituent of fenugreek were downloaded from PubChem Website.

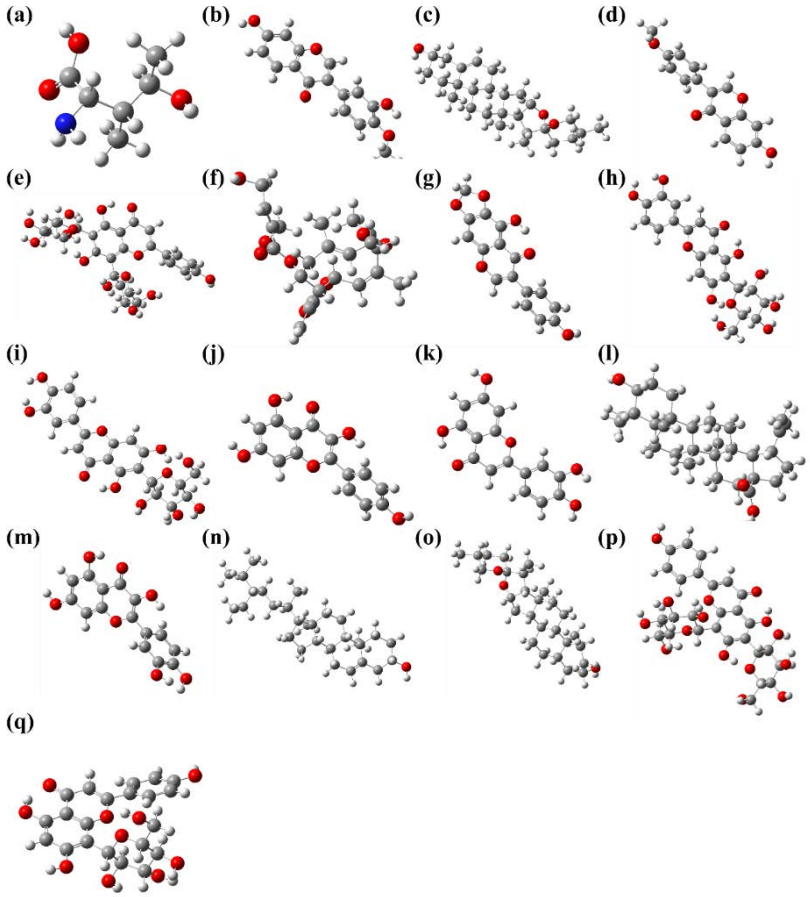

Fig. 1. Molecular structure of **(a)** 4-Hydroxyisoleucine (PubChem ID: 2773624), **(b)** Calycosin (5280448), **(c)** Diosgenin (99474), **(d)** Formononetin (5280378), **(e)** Schaftoside (442658), **(f)** Hiyodorilactone A (5281471), **(g)** Irolone (5281779), **(h)** Isoorientin (114776), **(i)** Isovitexin (162350), **(j)** Kaempferol (5280863), (k) Luteolin (5280445), **(l)** Mairin (64971), (m) Quercetin (5280343), **(n)** Sitosterol (222284), **(o)** Tigogenone (99516), **(p)** Vicenin-2 (442664), and **(q)** Vitexin (5280441).

J. Mex. Chem. Soc. **2025**, *69*(4)
Regular Issue

ISSN-e 2594-0317

Molecular docking

The interaction between a ligand and its receptor has been analyzed using molecular docking, which reveals that ligand-receptor binding occurs via various non-covalent interactions between the protein and the ligand. A single dominant form (at physiological pH) was chosen for the study to ensure consistency in the computational approach. The default pH of 7.0 was used throughout the study. Several software tools are utilized for docking studies. AutoDock Vina Programs and MGL Python-based tools have been employed to investigate the effect of constituent of Fenugreek over **CCHFV**.[29-31]

Molecular dynamics simulation

To examine the influence of Fenugreek constituents on CCHFV, molecular dynamics (MD) simulations were conducted using the Gromacs 2024 software suite.[32] The simulations employed the CHARMM27 force field, which incorporates specialized terms for addressing dihedral potentials. This force field utilizes the TIP3P water model with Lennard-Jones interactions for accurate molecular representation.[33] The simulations used an all-atom force field designed for proteins, with the proteins solvated homogeneously within a cubic box containing water molecules modeled by point charges. Periodic boundary conditions were applied to eliminate boundary artifacts, and an appropriate number of counter ions were introduced to neutralize the system.[34]

To maintain bond lengths, including hydrogen bonds, a constraint-solving algorithm was employed. Simulations were performed under an NVT ensemble (constant number of particles, volume, and temperature) at 300K, using Berendsen temperature coupling. This was followed by an NPT ensemble (constant number of particles, pressure, and temperature) where pressure control was achieved via Parrinello-Rahman pressure coupling with a time constant of 0.1 ps and a pressure of 1 bar. The cutoff radii for short-range electrostatic and van der Waals interactions were set at 1.2 nm. The simulation utilized a time step of 2 fs and a Fourier spacing of 0.16 nm. The MD simulation ran for 4000 ps (4ns), with coordinates saved every 10 ps for post-simulation analysis.

Results and discussion

A docking analysis was conducted for each key constituent of fenugreek with the Crimean-Congo Hemorrhagic Fever Virus (CCHFV). [35, 36] The most energetically stable complexes between fenugreek constituents and CCHFV were examined to identify the amino acids involved in the interactions. The findings, detailing these interactions, are presented in Table 1.

Table 1. Analysis of the interaction of key constituents of fenugreek with the Crimean-Congo Hemorrhagic Fever Virus (CCHFV).

Components	Affinity	Final Intermolecular Energy	Final Total Internal Energy	Torsional Free Energy	Unbound System's Energy
4-Hydroxyisoleucine	-4.7007	-5.830	-0.277	1.237	-0.170
Calycosin	-7.7641	-9.132	-0.377	1.362	-0.383
Diosgenin	**-9.4385**	**-9.714**	**0.000**	**0.276**	**0.000**
Formononetin	-7.5344	-9.031	0.076	1.101	-0.319
Schaftoside	-8.794	-13.420	-1.900	4.627	-1.900
HiyodorilactoneA	-8.1377	-11.260	-2.497	3.806	-1.822
Irolone	-8.1980	-9.139	-0.210	0.959	-0.192
Isoorientin	-8.0093	-11.220	-1.098	3.271	-1.054

J. Mex. Chem. Soc. **2025**, *69*(4)
Regular Issue

ISSN-e 2594-0317

Components	Affinity	Final Intermolecular Energy	Final Total Internal Energy	Torsional Free Energy	Unbound System's Energy
Isovitexin	-8.5264	-11.290	-1.079	3.240	-0.605
Kaempferol	-8.3274	-9.615	-0.279	1.460	-0.106
Luteolin	-8.1310	-9.392	-0.275	1.393	-0.331
Mairin	-9.0790	-10.690	-0.302	1.592	-0.326
Quercetin	-7.7339	-9.308	-0.271	1.582	-0.262
Sitosterol	-8.1720	-11.290	-1.402	3.105	-1.421
Tigogenone	**-9.6047**	**-9.885**	**0.000**	**0.281**	**0.000**
Vicenin2	**-9.3007**	**-13.910**	**-1.828**	**5.709**	**-0.732**
Vitexin	-9.1962	-12.310	-1.154	3.494	-0.778

Table 1 presents molecular docking results, summarizing key interaction energies for key constituents of fenugreek with the CCHFV protein. The data includes values for binding affinity, final intermolecular energy, total internal energy, torsional free energy, and unbound system's energy. The constituents of fenugreek show a range of binding affinities, with Tigogenone (-9.6047 kcal/mol) having the highest affinity, indicating stronger binding with CCHFV protein whereas 4-Hydroxyisoleucine has the weakest affinity (-4.7007 kcal/mol).

Furthermore, Schaftoside shows the lowest final intermolecular energy (-13.420 kcal/mol), indicating strong interactions with the CCHFV protein whereas 4-Hydroxyisoleucine again shows the weakest interaction (-5.830 kcal/mol).

On inspecting the Total Internal Energy values. Most constituents of fenugreek with the CCHFV protein have negative values, but Diosgenin, and Tigogenone show zero internal energy changes, indicating no deformation or strain upon binding.

Interestingly, the Torsional Free Energy gave some relevant information too. Vicenin2 (5.709 kcal/mol) and Schaftoside (4.627 kcal/mol) exhibit the highest torsional free energies, implying more flexibility or conformational changes during binding. In contrast, Diosgenin and Tigogenone have zero torsional free energy, suggesting rigid structures.

Furthermore, Sitosterol and HiyodorilactoneA show significant energy differences when unbound (-1.421 kcal/mol and -1.822 kcal/mol respectively), while Diosgenin, and Tigogenone have zero unbound energy, indicating no energy difference between bound and unbound states.

Eventually, constituents of Fenugreek like Diosgenin, Tigogenone and Vicenin2 exhibit strong binding affinities with minimal conformational changes, whereas Vicenin2 show strong intermolecular interactions but high flexibility.

Interaction of various constituents of Fenugreek with CCHFV

The interactions of seventeen distinct constituents of fenugreek with the CCHFV protein have been investigated and are summarized in Table S1 (see supporting information).[37] Each constituent's interaction is subsequently detailed individually for a comprehensive analysis.

4-Hydroxyisoleucine against CCHFV

The binding of 4-Hydroxyisoleucine to the active sites of CCHFV was evaluated and documented. It forms interactions with chain A of CCHFV via Gly409 and Leu335 residues. Specifically, a significant hydrogen bond with Gly409 is observed at a distance of 2.71 Å, while a hydrophobic interaction occurs with Leu335 at 3.59 Å.

J. Mex. Chem. Soc. **2025**, *69*(4)
Regular Issue

ISSN-e 2594-0317

Calycosin against CCHFV

The binding of Calycosin to CCHFV's active sites has been studied and presented. It forms interactions with chain A through residues such as Ile305, Ile374, Ile449, Ala451, Ala300, Ser387, and Thr411. Notable hydrogen bond distances include 3.10, 2.13, 2.60, and 2.69 Å with Ala300, Ser387, and Thr411, respectively. Hydrophobic interactions with Ile305, Ile374, Ile449, and Ala451 are found at 3.93, 3.59, 3.77, and 3.81 Å, respectively.

Diosgenin against CCHFV

The interaction of Diosgenin with the binding sites of CCHFV has been analyzed. It forms bonds with chain A via residues Ile305, Arg373, Tyr64, Ile449, and Ala451. Prominent hydrogen bonds are formed with Ile305 and Arg373 at 2.07 and 2.74Å, respectively. Hydrophobic contacts occur with Tyr64, Ile449, and Ala451 at 3.91, 3.21, and 3.51 Å, respectively.

Formononetin against CCHFV

The binding of Formononetin to CCHFV's active sites has been studied and outlined. It interacts with chain A via Arg373, Thr382, Arg385, Ile305, and Ile449. Notable hydrogen bond distances are 2.67, 2.26, and 3.49 Å with Arg373, Thr382, and Arg385, respectively. Hydrophobic contacts with Ile305, Arg373, Arg385, and Ile449 are measured at 3.80, 3.57, 3.84, and 4.49 Å, respectively.

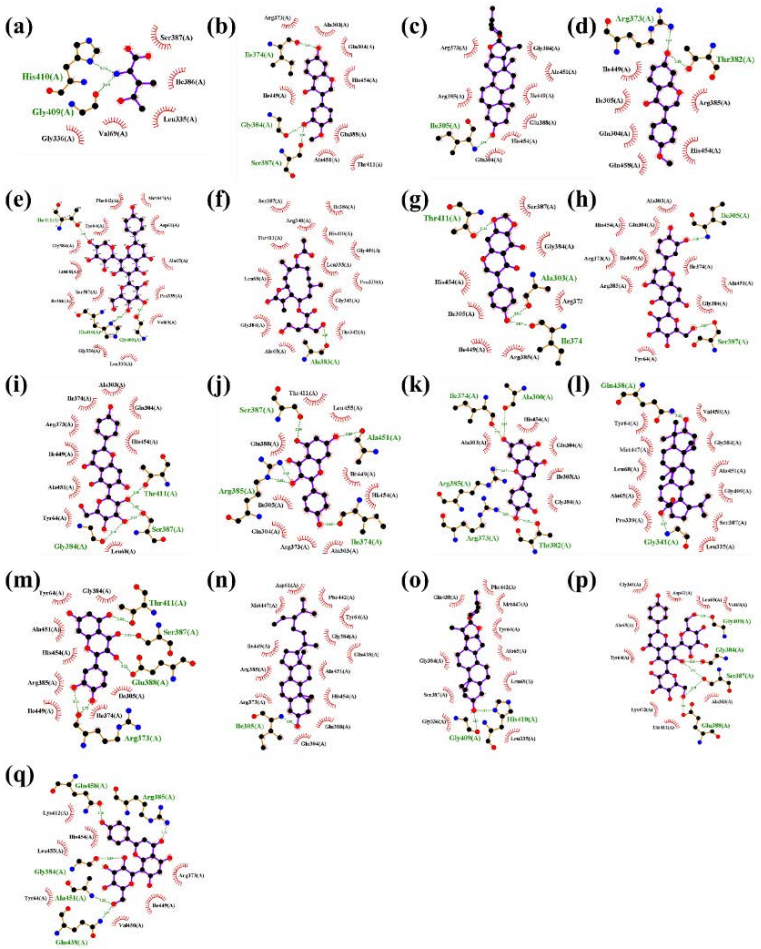

Fig. 2. Ligand-Protein Complex for **(a)** 4-Hydroxyisoleucine, **(b)** Calycosin, **(c)** Diosgenin, **(d)** Formononetin, **(e)** Schaftoside, **(f)** HiyodorilactoneA, **(g)** Irolone, **(h)** Isoorientin, **(i)** Isovitexin, **(j)** Kaempferol, **(k)** Luteolin, **(l)** Mairin, **(m)** Quercetin, **(n)** Sitosterol, **(o)** Tigogenone, **(p)** Vicenin2 and **(q)** Vitexin with CCHFV protein.

J. Mex. Chem. Soc. **2025**, *69*(4)
Regular Issue

ISSN-e 2594-0317

Schaftoside against CCHFV

Schaftoside interacts strongly with the CCHFV protein through a combination of hydrophobic interactions and hydrogen bonding, ensuring stable binding. Hydrophobic contacts with Asp-61, Tyr-64, and Phe-442 (3.44–3.69 Å) enhance ligand retention, with Phe442 likely contributing pi-stacking interactions for additional stability. Hydrogen bonds with Gly341, Ser387, Gly409, His410, and Thr411 further reinforce binding. Ser387 forms multiple bonds, while GLY-409 and THR-411 (both 2.09 Å) provide strong stabilization. His410's imidazole may offer electrostatic support, while Gly residues ensure flexibility for ligand accommodation.

HiyodorilactoneA against CCHFV

The binding of HiyodorilactoneA to CCHFV has been explored. It interacts with chain A via Thr342, Ala65, Leu335, Pro339, and Ile386. A key hydrogen bond with Thr342 is formed at a distance of 3.90 Å, while hydrophobic interactions with Ala65, Leu335, Pro339, Thr342, and Ile386 are noted at 3.63, 3.77, 3.89, 3.70, and 3.76 Å, respectively.

Irolone against CCHFV

The binding of Irolone to the active sites of CCHFV was analyzed and reported. It interacts with chain A via Ser387, Thr411, Ile305, Ile449, and Ala451. Major hydrogen bonds with Ser387 and Thr411 are formed at 3.00 Å and 2.17 Å, respectively. Hydrophobic interactions with Ile305, Ile449, and Ala451 are found at 3.83, 3.45, and 3.91 Å, respectively.

Isoorientin against CCHFV

The binding of Isoorientin to CCHFV's active sites has been studied. It forms interactions with chain A via Ile305, Gly384, Ser387, Thr411, Ile374, and Ile449. Significant hydrogen bond distances are observed at 2.11, 2.15, 2.54, and 3.32 Å with Ile305, Gly384, Ser387, and Thr411, respectively. Hydrophobic contacts with Ile374 and Ile449 are at 3.62 and 3.66 Å, respectively.

Isovitexin against CCHFV

The interaction of Isovitexin with CCHFV's active sites has been studied. It interacts with chain A via Ala233, Gly384, Ser387, Thr411, Ile374, Ile449, and Ala451. Notable hydrogen bond distances include 2.33, 2.99, 1.82, and 2.28 Å with Ala233, Gly384, Ser387, and Thr411. Hydrophobic contacts occur with Ile374, Ile449, and Ala451 at 3.46, 3.66, and 3.77 Å, respectively.

Kaempferol against CCHFV

The binding of Kaempferol to CCHFV has been studied. It interacts with chain A via Ala300, Arg385, Ser387, Ile374, Thr411, Ile449, and His454. Major hydrogen bonds are formed at 3.31, 2.46, and 2.88 Å with Ala300, Arg385, and Ser387, while hydrophobic interactions with Ile374, Thr411, Ile449, and His454 are observed at 3.90, 3.69, 3.66, and 3.53 Å, respectively.

Luteolin against CCHFV

The interaction of Luteolin with CCHFV's binding sites has been explored. It forms bonds with chain A via Ala303, Ile305, Arg373, Thr382, His454, Gln304, and Ile374. Major hydrogen bond distances include 3.63, 4.04, 2.93, and 3.12 Å with Ala303, Ile305, Arg373, and Thr382. Hydrophobic contacts with Gln304, Arg373, and Ile374 are observed at 3.85, 3.60, and 3.92 Å, respectively.

Mairin against CCHFV

The interaction of Mairin with CCHFV's active sites has been analyzed. It binds to chain A via Gly341, Gln438, Ala451, Tyr66, and Val69. Key hydrogen bonds are found at 3.27, 3.13, and 2.69 Å with Gly341, Gln438, and Ala451, while hydrophobic interactions with Tyr66, Val69, and Ala451 are noted at 3.66, 3.95, and 3.24 Å, respectively.

J. Mex. Chem. Soc. **2025**, *69*(4)
Regular Issue

ISSN-e 2594-0317

Quercetin against CCHFV

The interaction of Quercetin with CCHFV has been examined. It binds to chain A via Tyr64, Arg385, Ser387, Glu388, Thr411, and Ile449. Major hydrogen bonds occur at 2.94, 2.73, 2.53, 2.88, and 1.84 Å with respective residues, while hydrophobic interaction with Ile449 is noted at 3.75 Å.

Sitosterol against CCHFV

The binding of Sitosterol to CCHFV's active pockets has been analyzed. It interacts with chain A via Ala303, Ile305, Tyr64, Ile449, and Ala451. Significant hydrogen bonds are formed with Ala303 and Ile305 at 3.21 and 2.15 Å, respectively. Hydrophobic interactions occur with Tyr64, Ile449, and Ala451 at 3.49, 3.29, and 3.36 Å, respectively.

Tigogenone against CCHFV

The interaction of Tigogenone with the binding pockets of CCHFV has been reported. It interacts with chain A through Ala65 and Phe442. Significant hydrogen bonds are noted at 3.87 and 3.47 Å with Ala65 and Phe442, respectively.

Vicenin2 against CCHFV

The binding of Vicenin2 to CCHFV's active sites has been studied. It interacts with chain A via Leu335, Ala383, Gly384, Ser387, Thr411, Asp61, Tyr64, and Ala65. Major hydrogen bond distances are 3.75, 2.48, 3.44, 3.14, and 3.13 Å with respective residues. Hydrophobic interactions occur with Asp61, Tyr64, and Ala65 at 3.88, 4.00, and 3.51 Å, respectively.

Vitexin against CCHFV

The interaction of Vitexin with CCHFV has been evaluated. It binds to chain A via Tyr64, Arg373, Gly384, Arg385, Gln438, Ala451, His454, and Ile449. Major hydrogen bonds occur at 3.12, 2.24, 2.97, 1.84, 2.13, 2.50, and 3.04 Å with respective residues, while hydrophobic interactions with Arg373, Ile449, and His454 are found at 4.00, 3.49, and 3.34 Å, respectively.

Fig. S2 particularly shows the three most stable Ligand-Protein Complexes among all ligands. These complexes are for Diosgenin, Tigogenone and Vicenin2 for CCHFV protein.

Non-Covalent Interaction (NCI) plot

The Non-Covalent Interaction (NCI) plot is a valuable tool for analyzing various non-covalent interactions present in macromolecules.[19,22,30,38] The reduced density gradient is to quantify the parameters associated with non-covalent interactions in the NCI plot.[38] In this study, the NCI plot was employed to investigate the interactions of Diosgenin, Tigogenone, and Vicenin2 within the active site of the CCHFV protein. For this analysis, the docking poses with the lowest binding energies were selected, and Pymol software was used to identify close interactions within a distance of 3.5 Å. Key residues from the CCHFV protein, along with Diosgenin, Tigogenone, and Vicenin2, were chosen to generate the NCI plot.

Fig. 4 illustrates the NCI plots and the associated non-covalent interactions for Diosgenin, Tigogenone, and Vicenin2 in complex with the CCHFV protein. The color scheme used in the isosurfaces is as follows: blue indicates strong attractive interactions, green represents moderately strong interactions such as hydrogen bonding, π-π interactions, and van der Waals (vdW) forces, while red signifies repulsive interactions. The NCI plots predominantly show a mix of green and blue regions, indicating the presence of both electrostatic and dispersion interactions. Fig. 4(a), (b), (c) display RDG plots from the NCI analysis of the docking poses for Diosgenin, Tigogenone, and Vicenin2 with the CCHFV protein. These plots reveal that the binding strength primarily arises from hydrogen bonding and vdW interactions, as reflected by the dominance of blue and green colors in the plots.

Fig. 4(d) illustrates the isosurface extraction from the NCI analysis, highlighting key hydrogen bonds formed between Diosgenin and the CCHFV protein. Notably, these bonds occur with Ile305 and Arg373 at distances of 2.07 Å and 2.74 Å, respectively, corroborating the interactions depicted in Fig. 2. Moving to Fig. 4(e) and 4(f), they show the NCI isosurface extractions for Tigogenone and Vicenin-2, respectively, in complex with the CCHFV protein. In Fig. 4(e), significant hydrogen bonds are observed between Tigogenone and Ala65 (3.87 Å) and Phe442 (3.47 Å). Fig. 5(f), on the other hand, details Vicenin-2's interaction with CCHFV chain A through residues Leu335, Ala383, Gly384, Ser387, Thr411, Asp61, Tyr64, and Ala65. Key hydrogen bond distances here

J. Mex. Chem. Soc. **2025**, *69*(4)
Regular Issue

ISSN-e 2594-0317

include 3.75, 2.48, 3.44, 3.14, and 3.13 Å. These NCI plots offer a comprehensive view of the intermolecular interactions between the ligands and the CCHFV receptor, providing insights into the nature of their binding.

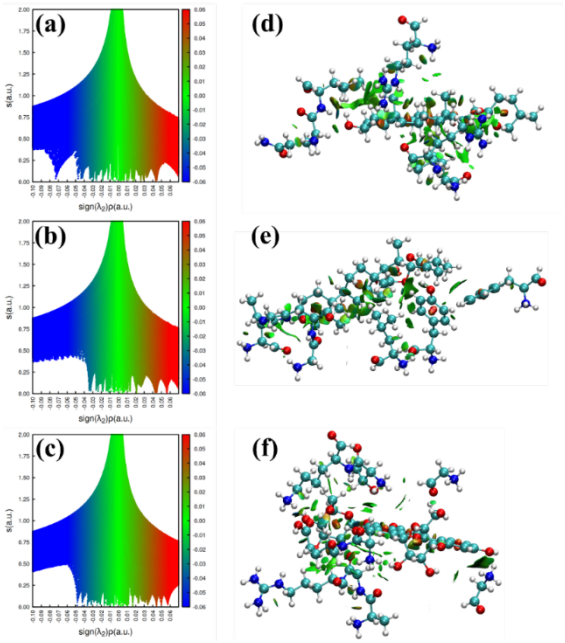

Fig. 4. The RDG plots along with its corresponding isosurface visualizations from the RDG analysis from the NCI analysis for the docking configurations of Diosgenin, Tigogenone, and Vicenin2 with the CCHFV protein are shown in figures **(a & d)**, **(b & e)**, and **(c & f)**, respectively.

Molecular dynamic studies

The use of molecular dynamics (MD) simulation allows for real-time observation of ligand-protein binding interactions over a specified duration, enabling the prediction of the ligand's conformational stability within the protein's binding site. In this study, 2 ns MD simulations were performed to assess the stability of Diosgenin, Tigogenone, and Vicenin-2, key constituents of fenugreek, when docked into CCHFV protein binding pocket.

The simulation results indicated that these compounds maintained a stable conformation within the protein's binding site throughout the simulation. The analysis of the root mean square deviation (RMSD) of the protein backbone showed that the protein complexes formed with Diosgenin, Tigogenone, and Vicenin-2 reached a stable equilibrium at the same time, signifying that these ligands provide structural stability to the protein.

Moreover, the comparison of the protein-ligand complexes with the unbound protein revealed that the presence of these ligands increased the overall stability of the protein. This suggests that Diosgenin, Tigogenone, and Vicenin-2 not only fit well into the binding pocket but also interact effectively with the surrounding amino acids, enhancing the rigidity of the protein structure.

Hydrogen bond formation

The hydrogen bond formation between Diosgenin, Tigogenone, Vicenin-2, and the CCHFV protein was evaluated over the 4000 ps molecular dynamics trajectory (Fig. 5). The Diosgenin-CCHFV complex showed the formation of two hydrogen bonds, with one remaining stable throughout the simulation. In the case of the Tigogenone-CCHFV complex, a single hydrogen bond was observed, which was consistently maintained during the simulation period. For the Vicenin-2-CCHFV complex, four hydrogen bonds were formed, with two or three bonds remaining stable throughout the simulation. It can be inferred that the stability of these complexes is largely driven by persistent hydrogen bonding, especially for the Vicenin-2-CCHFV complex.

J. Mex. Chem. Soc. **2025**, *69*(4)
Regular Issue

ISSN-e 2594-0317

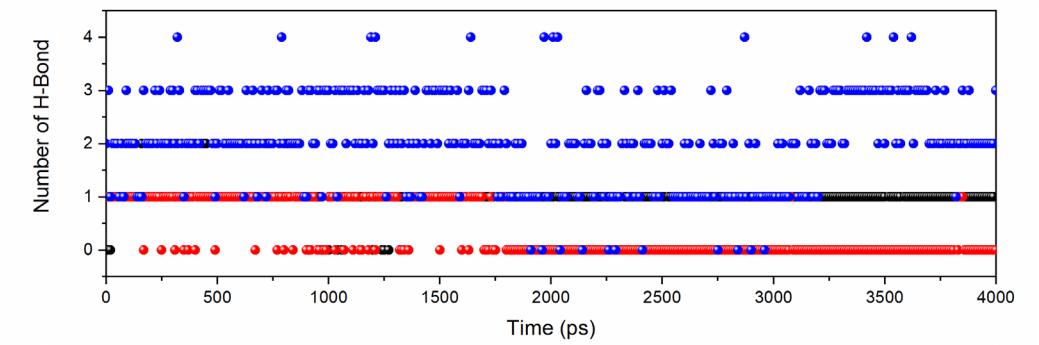

Fig. 5. Number of hydrogen bond formations of Diosgenin (Black), Tigogenone (Red), and Vicenin2 (Blue) with the CCHFV protein during a 4000 ps MD simulation.

Analysis of principal components

Fig. 6(a) shows the 2D projection of the first two eigenvectors. In the Diosgenin-CCHFV complex, it was observed that Diosgenin-CCHFV exhibited comparable diversity in conformations during the simulations (shown in black) with Tigogenone (red), and Vicenin2 (blue) in complex with the CCHFV protein. It was widely clustered in the range of −10 to 10. Fig. 6(b) shows that the eigenvalue of the Diosgenin (black), Tigogenone (red), and Vicenin2 (blue) in complex with the CCHFV protein are 18.75 nm2, 13.75 nm2 and 10 nm2, suggesting that the secondary structure of the Diosgenin-CCHFV complex underwent significant conformational changes throughout the 4 ns simulation, favouring the formation of a stable complex.

Gibbs free energy landscapes (FELs)

Fig. 7 illustrates the free energy landscapes (FELs) of the ligand-protein complexes involving (a) Diosgenin, (b) Tigogenone, and (c) Vicenin2 with the CCHFV protein, plotted as a function of two reaction coordinates or principal components (PCs). The FEL plots reveal distinct free energy distributions between the unbound and ligand-bound protein complexes. Despite these differences, the protein was still able to adopt energetically favorable and structurally stable conformations. The analysis of FELs indicates that the inclusion of small molecules influenced both the size and position of the sampled energy basins, contributing to stable equilibrium states.

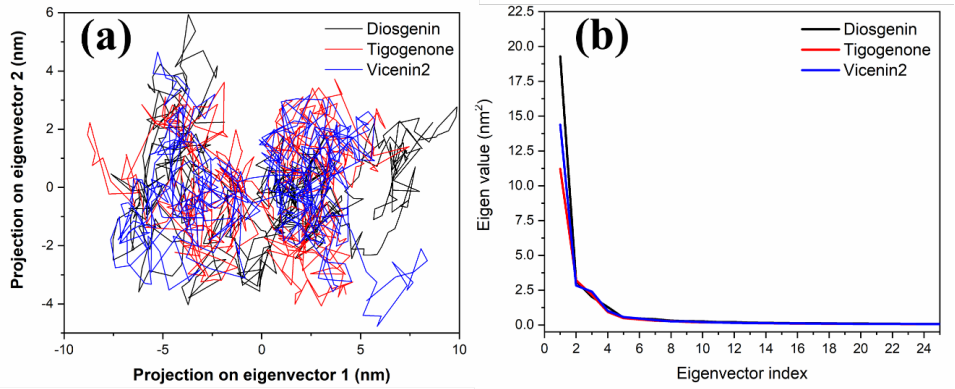

Fig. 6. (a) Principal component analysis (PCA) of the protein-ligand complexes: The collective motions of Diosgenin (black), Tigogenone (red), and Vicenin2 (blue) with the CCHFV protein were analyzed by projecting the MD trajectories onto two eigenvectors corresponding to the first two principal components. (b) The plot shows the first 25 eigenvectors versus their associated eigenvalues for Diosgenin (black), Tigogenone (red), and Vicenin2 (blue) in complex with the CCHFV protein.

J. Mex. Chem. Soc. **2025**, *69*(4)
Regular Issue

ISSN-e 2594-0317

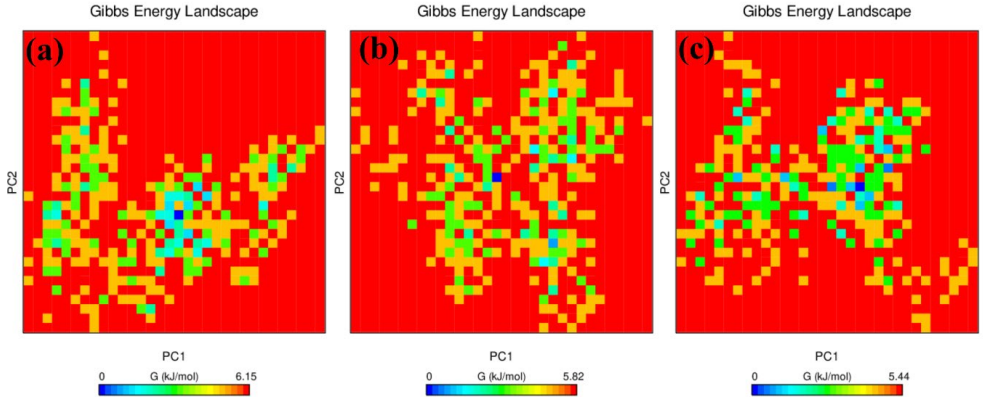

Fig. 7. Gibbs Free Energy Landscape for Ligand-Protein Complex of **(a)** Diosgenin, **(b)** Tigogenone and **(c)** Vicenin2 with CCHFV protein as a function of two reaction coordinates or principal components (PCs).

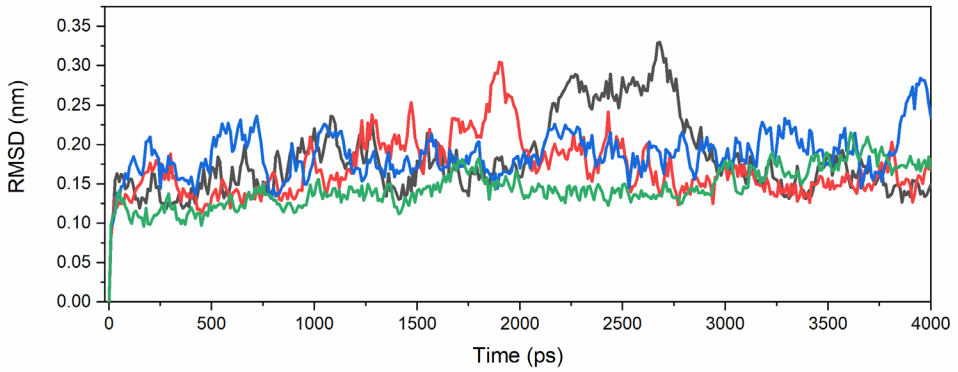

Fig. 8. RMSD Plot for Ligand-Protein Complex of Diosgenin (Black), Tigogenone (Red) and Vicenin2 (Blue) with CCHFV protein and separate protein (Green).

Root mean square deviation (RMSD) Plot

Fig. 8 presents the RMSD plot for the ligand-protein complexes of Diosgenin, Tigogenone, and Vicenin-2 with the CCHFV protein over a 4000 ps simulation. The CCHFV protein alone displayed an average backbone RMSD of approximately 1.25 Å. In comparison, the Diosgenin, Tigogenone, and Vicenin-2 complexes with the CCHFV protein exhibited average backbone RMSD values of around 1.5 Å, 1.4 Å, and 1.7 Å, respectively.

In summary, the MD simulations strongly indicate that Diosgenin, Tigogenone, and Vicenin-2 bind stably within the CCHFV protein's binding site. Their presence not only stabilizes the protein-ligand complexes but also imparts additional stability to the protein itself. These findings support the hypothesis that these fenugreek constituents could potentially serve as potential inhibitor and effectively interacting with the CCHFV protein.

Conclusions

Fenugreek is renowned for its medicinal and antiviral properties, which makes it a compelling candidate for combating viruses such as CCHFV. Due to the absence of approved treatments for CCHFV and the significant mortality associated with the virus, there is an urgent need for attention. The nucleoprotein of

J. Mex. Chem. Soc. **2025**, *69*(4)
Regular Issue

ISSN-e 2594-0317

CCHFV, which plays a key role in viral replication, has emerged as an attractive target for developing antiviral treatments. This research aimed to identify potential inhibitors of this nucleoprotein through virtual screening techniques. The study utilized a combination of docking and molecular dynamics (MD) simulations to evaluate seventeen active compounds derived from fenugreek for their ability to inhibit the nucleoprotein. Given that CCHFV is classified as a biosafety level-4 pathogen by WHO, which limits research in standard laboratories, in-silico approaches offer a safe and effective way to identify possible inhibitors. Based on the outcomes of the docking studies and MD simulations, Diosgenin, Tigogenone, and Vicenin-2 are suggested as potential inhibitors of the CCHFV nucleoprotein. These results indicate that compounds from fenugreek may serve as valuable candidates for the development of antiviral therapies targeting CCHFV.

Acknowledgments

SK thanks Magadh University, Bodh Gaya, Bihar, India for providing lab facility and SERB, Department of Science and Technology (DST), India (Grant No. SRG/2019/002284) for financial support.

References

1. Srinivasan, K. *Food Rev. Int.* **2006** *22*, 203. DOI: http://dx.doi.org/10.1080/87559120600586315.
2. Al-Habori, M.; Raman, A., in: *Phytotherapy Research: An International Journal Devoted to Pharmacological and Toxicological Evaluation of Natural Product Derivatives.* **1998** *12*, 233
3. Smith, M. *Alternative Medicine Review.* **2003** *8*, 20
4. Sun, W.; Shahrajabian, M. H.; Cheng, Q. *Mini Rev. Med. Chem.* **2021** *21*, 724. DOI: http://dx.doi.org/10.2174/1389557520666201127104907.
5. Singletary, K. W. *Nutr. Today.* **2017**, *52*, 93.
6. Aboubakr, H. A.; Nauertz, A.; Luong, N. T.; Agrawal, S.; El-Sohaimy, S. A.; Youssef, M. M.; Goyal, S. M. *J. Food Prot.* **2016**, *79*, 1001. DOI: http://dx.doi.org/10.4315/0362-028X.JFP-15-593.
7. Alu'datt, M. H.; Rababah, T.; Al-ali, S.; Tranchant, C. C.; Gammoh, S.; Alrosan, M.; Kubow, S.; Tan, T. C.; Ghatasheh, S. *J. Food Sci.* **2024**, *89*, 1835
8. Salam, S. G. A.; Rashed, M. M.; Ibrahim, N. A.; Rahim, E. A. A.; Aly, T. A. A.; Al-Farga, A. *Sci. Rep.* **2023**, *13*, 7032. DOI: http://dx.doi.org/10.1038/s41598-023-31888-y.
9. Haxhiraj, M.; White, K.; Terry, C. *Int. J. Mol. Sci.* **2024**, *25*, 6987. DOI: http://dx.doi.org/10.3390/ijms25136987.
10. Agrawal, S.; Sanap, S. N.; Bisen, A. C.; Biswas, A.; Choudhury, A. D.; Verma, S. K.; Jaiswal, S.; Narender, T.; Bhatta, R. S. *Bioanalysis.* **2023**, *15*, 711. DOI: http://dx.doi.org/10.4155/bio-2023-0074.
11. Ahmad, I.; Kuznetsov, A. E.; Pirzada, A. S.; Alsharif, K. F.; Daglia, M.; Khan, H. *Front. Chem.* **2023**, *11*, 1145974. DOI: http://dx.doi.org/10.3389/fchem.2023.1145974.
12. Konstantinidis, N.; Franke, H.; Schwarz, S.; Lachenmeier, D. W. *Molecules.* **2023**, *28*, 3460. DOI: http://dx.doi.org/10.3390/molecules28083460.
13. Arya, P.; Munshi, M.; Kumar, P. *Food Chemistry Advances.* **2023**, *2*, 100170.
14. Aghababaei, F.; Hadidi, M. *Pharmaceuticals.* **2023**, *16*, 1020. DOI: http://dx.doi.org/10.3390/ph16071020.
15. Whitehouse, C. A. *Antiviral Res.* **2004**, *64*, 145. DOI: http://dx.doi.org/10.1016/j.antiviral.2004.08.001.
16. Elaldi, N.; and Kaya, S. *J. Med. Microbiol. Infect. Dis.* **2014**, *4*, 1.
17. Swanepoel, R.; Gill, D. E.; Shepherd, A. J.; Leman, P. A.; Mynhardt, J. H.; Harvey, S. *Rev. Infect. Dis.* **1989**, *11, Suppl 4*, S794. DOI: http://dx.doi.org/10.1093/clinids/11.supplement_4.s794.

J. Mex. Chem. Soc. **2025**, *69*(4)
Regular Issue

ISSN-e 2594-0317

18. Deyde, V. M.; Khristova, M. L.; Rollin, P. E.; Ksiazek, T. G.; Nichol, S. T. *J. Virol.* **2006**, *80*, 8834. DOI: http://dx.doi.org/10.1128/JVI.00752-06.
19. Kumar Panja, S.; Kumar, S.; Fazal, A. D.; Bera, S. *J. Photochem. Photobiol. A Chem.* **2023**, *445*, 115084. DOI: http://dx.doi.org/10.1016/j.jphotochem.2023.115084.
20. Kumar Panja, S.; and Kumar, S. *J. Mol. Liq.* **2023**, *375*, 121354. DOI: http://dx.doi.org/10.1016/j.molliq.2023.121354.
21. Kumar, S.; Prajapat, A.; Panja, S. K.; Shukla, M., in: *Green Chemical Synthesis with Microwaves and Ultrasound*. **2024,** 1.
22. Kumar Sada, P.; Kaur Jassal, A.; Bar, A.; Kumar, P.; Srikrishna, S.; Kumar, S.; Kumar Singh, A.; Lee, Y.; Singh, L.; Rai, A. *Microchem. J.* **2024**, *207*, 111710. DOI: http://dx.doi.org/10.1016/j.microc.2024.111710.
23. Panja, S. K.; Kumar, S.; Haddad, B.; Patel, A. R.; Villemin, D.; Amine, H.-M.; Bera, S.; Debdab, M. *Physchem.* **2024**, *4*, 369. DOI: http://dx.doi.org/10.3390/physchem4040026.
24. Srivastava, S.; Kumar, S.; Sharma, P. K.; Rustagi, S.; Mohanty, A.; Donovan, S.; Henao-Martinez, A. F.; Sah, R.; Franco-Paredes, C. *Health Sci. Rep.* **2024**, *7*, e70053. DOI: http://dx.doi.org/10.1002/hsr2.70053.
25. Kiefer, F.; Arnold, K.; Kunzli, M.; Bordoli, L.; Schwede, T. *Nucleic Acids Res.* **2009** *37*, D387. DOI: http://dx.doi.org/10.1093/nar/gkn750.
26. Waterhouse, A.; Bertoni, M.; Bienert, S.; Studer, G.; Tauriello, G.; Gumienny, R.; Heer, F. T.; de Beer, T. A. P.; Rempfer, C.; Bordoli, L.; Lepore, R.; Schwede, T. *Nucleic Acids Res*. **2018**, *46,* W296. DOI: http://dx.doi.org/10.1093/nar/gky427.
27. Madeira, F.; Madhusoodanan, N.; Lee, J.; Eusebi, A.; Niewielska, A.; Tivey, A. R. N.; Lopez, R.; Butcher, S. *Nucleic Acids Res.* **2024**, *52*, W521. DOI: http://dx.doi.org/10.1093/nar/gkae241.
28. Muhamad, F.; Ahmad, R. B.; Asi, S.; Murad, M. N. *J. Phys. Conf. Ser.* **2018,** *1019*, 012085.
29. Kumar, S., J. Serb. Chem. Soc. 2023 88, 381 DOI: http://dx.doi.org/10.2298/jsc220921087k.
30. Kumar, S.; and Panja, S. K. *Theor. Chem. Acc.* **2023**, *142*, 126. DOI: http://dx.doi.org/10.1007/s00214-023-03073-x.
31. Trott, O.; and Olson, A. J. *J. Comput. Chem.* **2010**, *31*, 455. DOI: http://dx.doi.org/10.1002/jcc.21334.
32. Berendsen, H. J.; van der Spoel, D.; van Drunen, R. *Comput. Phys. Commun.* **1995**, *91*, 43.
33. Mark, P.; and Nilsson, L. *J. Phys. Chem. A.* **2001**, *105*, 9954.
34. Kumar, V.; Kumar, R.; Kumar, N.; Kumar, S. *Asian J. Chem.* **2023**, *35*, 991. DOI: http://dx.doi.org/10.14233/ajchem.2023.27594.
35. Ergonul, O. *Curr. Opin. Virol.* **2012**, *2*, 215. DOI: http://dx.doi.org/10.1016/j.coviro.2012.03.001.
36. Frank, M. G.; Weaver, G.; Raabe, V. *Emerg. Infect. Dis.* **2024**, *30*, 847. DOI: http://dx.doi.org/10.3201/eid3005.231646.
37. Tewari, A.; Singh, R.; Brar, J. K. *J. Phytopharm.* **2024**, *13*, 97. DOI: http://dx.doi.org/10.1016/j.sajb.2022.04.014.
38. Contreras-Garcia, J.; Johnson, E. R.; Keinan, S.; Chaudret, R.; Piquemal, J. P.; Beratan, D. N.; Yang, W. *J. Chem. Theory Comput.* **2011**, 7, 625. DOI: http://dx.doi.org/10.1021/ct100641a.